

Impulse Capacitor Discharge Welding of Hollow Structure Made of Nickel-Base Alloy^{*}

WANG Jianzhao (王剑钊), Peter Ohse[†], WU Su (吴甦)^{**}, Ulrich Diltthey[†]

Department of Industrial Engineering, Tsinghua University, Beijing 100084, China;

[†] Welding and Joining Institute, RWTH Aachen, Aachen 52062, Germany

Abstract: Future steam turbines will use hollow structures so that the turbine inlet temperature can be increased to improve the thermal efficiency. These hollow structures are made of the nickel-base alloy Inconel 6025 HT and consist of a wire mesh between two cover sheets. The cover sheets can be joined to the wire mesh by capacitor discharge welding due to its extremely short welding duration. The goal of this research is to investigate suitable welding parameters so that the weld spots form in an optimum way to increase the tensile shear strength and reduce spattering. Tensile shear tests, three-point bending tests, and micrographs were used to judge the joint quality of structures made with various welding parameters. The results show that the best welds are obtained with a transmission ratio of 1:200, welding energy of 70% to 95%, and electrode force of 7 to 9 MPa.

Key words: capacitor discharge welding; nickel-base alloy; hollow structure; tensile shear test; three-point bending test; micrographs

Introduction

Today, steam turbines are the most widely used means of generating electricity. Hot steam flows through a turbine which rotates a shaft to drive a generator. Higher pressure and higher temperature steam will result in higher turbine efficiencies. However, these two parameters are restricted by the turbine blade material properties. Conventional steam turbine materials, martensitic steels, cannot withstand more than approximately 620°C in the long run^[1,2].

One method allowing increased steam temperatures is to use a composite structure consisting of two cover sheets and an intermediate wire mesh layer in between.

These hollow structures can provide coolant flow channels with the fluid cooling the turbine and shaft surfaces which are subjected to high thermal stresses.

Common methods of manufacturing such composite structures include diffusion joining with an active filler metal, friction welding, and TIG welding. These processes often require long exposure times at high temperatures or high pressures, leading to grain coarsening in the microstructure or heavy plastic deformation near the joint^[3].

The cover sheets can be joined to the wire mesh by capacitor discharge welding to form lattice segments. The extremely short welding times of this process ensure that the thermal loads on the base material outside the joining zone are quite small. The cooling rate in some condition can be as high as 1×10^6 K/s with capacitor discharge welding^[4-6]. A more narrow heat affected zone and reduced welding distortion and residual stresses can be obtained with capacitor discharge welding due to its quick welding process^[7]. The heat

Received: 2006-08-23

* Supported by the DAAD (German Academic Exchange Service) and CSC (China Scholarship Council) on Tsinghua University/RWTH Aachen Joint Master Program

** To whom correspondence should be addressed.

E-mail: wusu@tsinghua.edu.cn; Tel: 86-10-62787698

input can be controlled by varying the capacitor bank voltage that changes the current pulse amplitude. The condensers ensure that the energy of different pulses is constant, resulting in stability of the welded joint quality^[8,9].

To produce high quality composite structures, the process parameters, such as the transmission ratio, the electrode force, and the welding energy, need to be optimized. Since the composite structure will be used in a steam turbine, tensile strength, bending strength, and spattering tendency are also important criteria for producing high quality welded joints.

Conventional martensitic materials are not very corrosion-resistant in a steam atmosphere. Nickel-base alloys exhibit exceptional resistance to oxidation and carburization at higher temperatures. Therefore, a nickel-base alloy is normally used for these hollow structures.

1 Experimental Setup

The cost of the energy storage capacitors required by capacitor discharge welding machines makes them considerably more expensive than alternating current machines. However, capacitor discharge welding is still an excellent technology for specific applications in which very large, short duration welding currents are more effective than smaller currents for longer times. Examples of these applications are when a weld must be made in close proximity to a heat-sensitive area such as a glass-to-metal seal or explosive compounds^[10].

Impulse capacitor discharge welding is characterized by low thermal impact on the joined parts compared with conventional resistance welding. The welding process duration is extremely short because the capacitor discharges very quickly (8-20 ms) through a pulse transformer that generates a high current and relatively low voltage. The cover sheets and wire mesh are fixed between two copper electrodes at a defined pressing pressure before the capacitor is discharged (Fig. 1). The contact points of the three layers each constitute a resistance for the current. Local heating and complete melting of the material occur at the contact points to bond the plate and the wire mesh together.

In the experiments, two cover sheets with an intermediate wire mesh layer between the sheets were welded with a capacitor discharge welding machine from Manfred Schlemmer GmbH. The operating parameters of the welding machine were as follows: Input

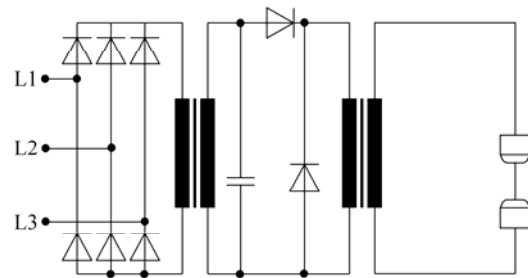


Fig. 1 Principle of the capacitor discharge welding test set-up

supply voltage is 400 V/50 Hz; connection power 30 kW; control voltage 230 V (AC)/24 V (DC); valve voltage 24 V (DC); charging voltage 0-3200 V, stepless; energy 0-20 kJ (100%), stepless; electrode force 0-30 kN (10 MPa), stepless.

The switchgear cabinet controlled the equipment and the capacitors. There were altogether six capacitors, each with a capacity of 640 μF , which could be alternatively switched. The hydraulic unit provided a maximum force of 30 kN. The impulse transformer transmission ratio could be changed on the instrument panel.

In a capacitor discharge welding machine, the welding time cannot be changed, only the transmission ratio can be changed, which indicates how quickly the capacitors will discharge into the weld. For a certain energy quantity existing in the capacitors, the maximum welding duration and thus minimum peak current value occur at a transmission ratio of 1:400, while the minimum welding time occurs at a transmission ratio of 1:100.

The two electrodes are key components of the resistance welding machine since they transmit the current and force to the workpiece. Different electrode materials affect the mechanical and electrical characteristics of the welding process, so the electrode material must be selected carefully. The requirement for good electrical and thermal conductivity can be fulfilled most economically with pure copper. However, copper does not adequately resist deformation and distortion in the workpiece, so the electrodes are normally made of copper alloys. These tests used flat 50 mm \times 50 mm electrodes made of a CuCrZr alloy.

In the wire mesh hollow structure, a so called "sandwich structure", both the cover sheet and the wire mesh were made of the nickel-base alloy Nicrofer 6025 HT (NiCr25FeAlY, designation according to VdTUV) which is a high-carbon, nickel-chromium-iron alloy with the micro-alloying elements titanium and zirconium together with aluminium and yttrium^[11].

The Chemical composition of Nicrofer 6025 HT is shown in Table 1:

Table 1 Chemical composition of Nicrofer 6025 HT (mass percentage)

	Cr	Fe	C	Mn	Si	Cu	Al	Ti	Y	Zr	Ni
Min	24.0	8.0	0.15	–	–	–	1.8	0.1	0.05	0.01	Rest
Max	26.0	11.0	0.25	0.1	0.5	0.1	2.4	0.2	0.12	0.10	Rest

The alloy exhibits exceptional resistance to oxidation at higher temperatures, even under cyclic conditions. It also possesses very good high temperature corrosion resistance in carburizing and oxidizing media as well as under “metal dusting” conditions due to its high chromium and aluminium content^[11].

The square mesh fabric (Fig. 2) was manufactured specially for these tests. The fabric mesh spacing w was about 2.2 mm with a wire diameter d of 0.8 mm. The fabric is quite uneven since the webbing process causes the chaining threads to exhibit larger curvatures as they bend around the strained shooting threads. This heterogeneity causes the chaining and shooting threads to be characterized by different rigidities in the thickness direction in the hollow structure.

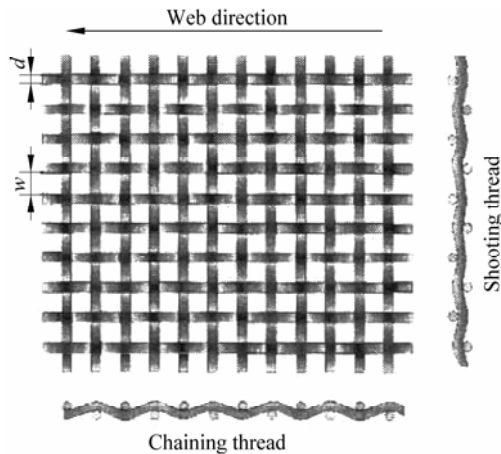


Fig. 2 Schematic of the mesh fabric

For the tensile shear tests, the cover sheets were made into 100 mm × 50 mm rectangles on a cutting machine. The intermediate wire mesh layer was 50 mm × 50 mm. The cover sheets were arranged such that one sheet extended to the right 50 mm while the other extended to the left 50 mm. In the tensile shear tests, the tensile force was applied in the direction of the shooting threads. For the three-point bending tests, the cover sheets and wire mesh had the same dimensions of 150 mm × 50 mm.

The long side of the cover sheet was placed parallel

to the rolling direction to exclude any influence of the texture. The optimal welding parameters were measured with the shooting direction of the wire mesh always parallel to the longer side of the sample.

The welded composite materials were tested with tensile shear tests and three-point bending tests conducted on the same testing machine manufactured by Instron (High Wycombe, United Kingdom)^[12]. The testing machine had digital control connected to a computer. The machine and computer controls were used to vary the drop speed, maximum drop path, and maximum compressive or tensile force. The measured forces and positions were recorded on a computer.

2 Results and Discussion

The welding experiments are implemented with the capacity of all six capacitors ($6 \times 640 \mu\text{F}$). The parameters varied in the experiments were the transmission ratio (1:100, 1:200, 1:400) which controls the welding time, the electrode force or pressure, and the welding energy.

The welding energy is indicated as a percentage of the maximum energy of 20 kJ. The resulting pressure depended on the applied electrode force and the area. In the experiments, the maximum electrode force of 30 kN corresponded to a pressure of 10 MPa.

The electrode force is lowered from 9 MPa to 4 MPa in steps of 0.5 MPa. For each pressure, the welding energy was increased from 30% to 95% in steps of 5%. To ensure reproducibility, three pieces were made for each welding parameter setting.

For the typical tensile shear test result shown in Fig. 3, the deformation rate was 5 mm/min with the tensile force applied steadily. The stretching of the composite structure and the applied force were simultaneously recorded by the computer.

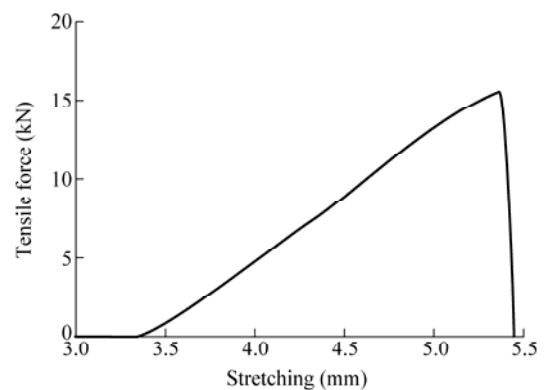


Fig. 3 Typical stress-strain curve for a composite structure (welding energy 90%, electrode force 9 MPa, transmission ratio 1:200)

All specimens showed similar stress-strain behavior as illustrated in Fig. 3. At the beginning of the tensile tests, the tensile force increased very slowly due to play in the tensile test equipment. Then, the tensile force increased steadily up to a maximum after which the tensile force abruptly fell to zero.

Figure 4 illustrates the variation of the tensile strength of the welded joints for the various welding parameter settings. A distinct optimal parameter range for a transmission ratio of 1:200 is marked by an ellipse in Fig. 4.

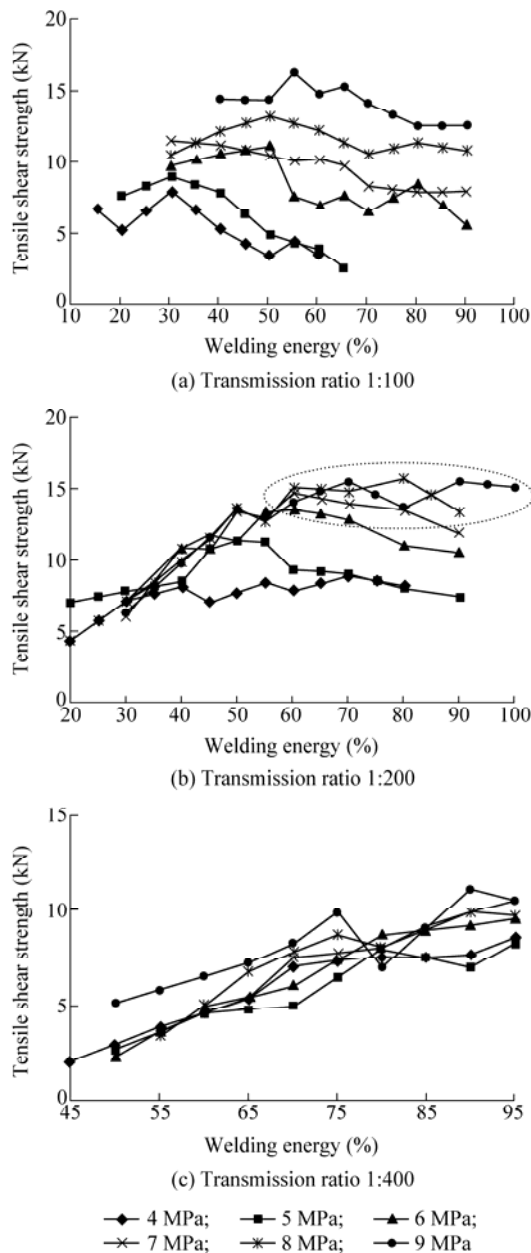


Fig. 4 Tensile test results for the various welding parameter settings

Generally, the strength initially increases with increasing welding energy before dropping when welding spattering occurs. Two effects were observed as the welding energy increases. First, higher welding energies create larger weld nugget so that the resulting tensile strengths are higher. At higher welding energies, the welding pressure or electrode force has to be increased so that the composite structure and the electrode will not stick together. However, as pressure increases, the resistance between the cover sheets and the wire mesh decreases, which reduces the tensile shear strength.

Micrographs were used to observe the microstructure of the welded joint. Before the micrographs were taken, nitric acid or vitriol acid was used to etch the sample. The micrographs are very time consuming, so only one sample at the optimal parameter settings was photographed.

The two micrographs shown in Fig. 5 were taken from the shooting direction of the wire mesh. Figure 5a shows much spattering in the weld zone between the wire mesh and the cover sheets. Figure 5b is a better weld with little spattering.

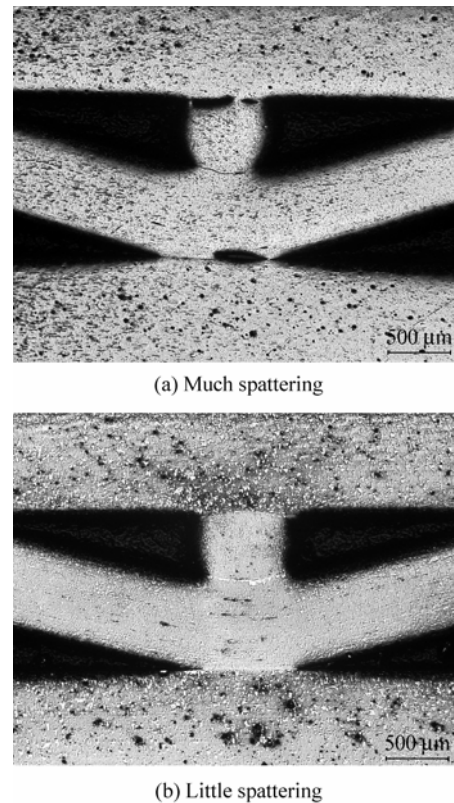
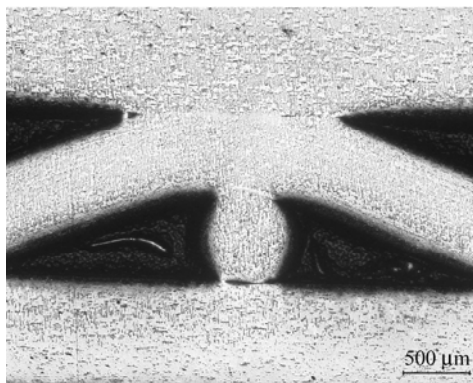
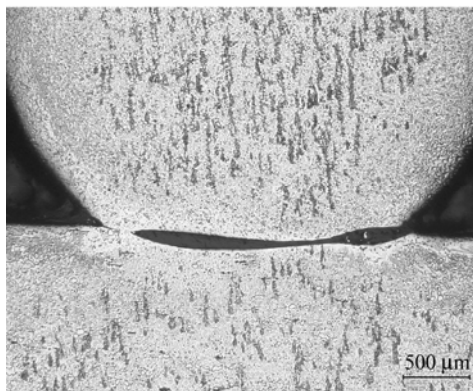


Fig. 5 Micrographs in the shooting direction (electrode force 9 MPa, energy 90%, transmission ratio 1:200)

The micrographs shown in Fig. 6 taken from the wire mesh chaining direction shows the clearly larger curvature. Figure 6b with a larger resolution shows that the joint between the wire thread and the cover sheet is not complete. Such joints will definitely fail earlier in the tensile shear tests.



(a) Lower resolution



(b) Larger resolution

Fig. 6 Micrographs in the chaining direction (electrode force 9 MPa, energy 90%, transmission ratio 1:200)

The three-point bending tests used a deformation rate of 3 mm/min and a maximum punching force of 600 kN. The tests were terminated after a process path of 12 mm. The punching force and the process path were simultaneously recorded during the tests.

The three-point bending tests were implemented for each parameter setting of the optimal parameter range found in the tensile shear tests. All the results shown in Fig. 7 are the average of test results of two samples welded with the same parameter settings. The variation of the welded joints strength shown in Fig. 7 is similar to the results of the tensile shear tests.

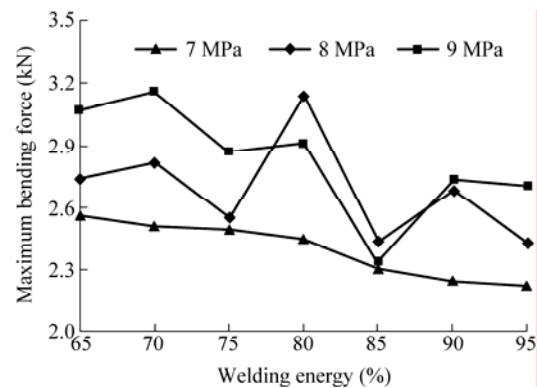


Fig. 7 Three-point bending test results (transmission ratio 1:200)

3 Conclusions

The tensile shear tests and the three-point bending tests show that the welds are stronger for transmission ratios of 1:100 and 1:200. However, spattering increases for the 1:100 transmission ratio due to its too high peak current value. For the 1:400 transmission ratio, the capacitor discharge welding machine is not sufficiently powerful to produce higher tensile strengths. Therefore, the 1:200 transmission ratio gives the best results for the material combination investigated in these experiments. The optimal welding energy is from 70% to 95%, while the electrode force is from 7 MPa to 9 MPa for the 1:200 transmission ratio.

The wire mesh is very uneven since the chaining threads exhibit larger curvatures due to bending during the production procedure than the shooting threads. Therefore, the chaining and shooting threads are characterized by different rigidities in thickness in the composite structure. These experiments only analyzed arrangements where the shooting thread was parallel to the longer side of the cover sheet with the shear measured in the direction of the shooting threads. Further research should investigate the weld strengths when the shooting thread is parallel to the shorter side of the cover sheet and the shear is measured in the direction of the chaining thread.

Acknowledgements

We thank the Welding and Joining Institute (ISF) at Aachen University of Technology for the laboratory facilities and the material for the hollow structures. The authors also gratefully

acknowledge the financial support of the Deutsche Forschungsgemeinschaft (DFG) within the Collaborative Research Center (SFB) project entitled "Thermally highly loaded, porous and cooled multi-layer-systems for combined cycle power plants".

References

- [1] Dilthey U, Ohse P, Piontek D. Welding of hollow structures made of high-temperature materials. *Welding and Cutting*, 2004, (3): 156-159.
- [2] Hagedorn G, Paul I. Innovative steam power plant technology—New solutions for the benefit of customers worldwide. In: Power Gen Europe '97. Madrid, Spain, 1997.
- [3] Matsugi K, Konishi M, Yanagisawa O, Kiritani M. Joining of spheroidal graphite cast iron to stainless steel by impact-electric current discharge joining. *Journal of Materials Processing Technology*, 2004, **150**: 300-308.
- [4] Zhai Q, Lei M, Xu J. Microstructure analysis on capacitor discharge welded Al₂O₃ fiber reinforced Al-matrix composites joint. *Transactions of the China Welding Institution*, 2005, **26**(8): 65-68. (in Chinese)
- [5] Xu J, Zhai Q, Yuan S. Energy-storage welding connection characteristics of rapid solidification AZ91D Mg Alloy Ribbons. *Journal of Materials Science and Technology*, 2004, **20**(4): 431-434.
- [6] Xu J, Zhai Q, Jiang Y. Energy-storage welding connection characteristics of rapidly solidified Cu-Co alloy foils. *Transactions of Nonferrous Metals Society of China*, 2004, **14**(4): 785-789.
- [7] Li M, Sun D, Qiu X, Sun D, Yin S. Microstructures and properties of capacitor discharge welded joint of TiNi shape memory alloy and stainless steel. *China Welding*, 2005, **14**(2): 95-100.
- [8] Zapol'skikh S N, Melyukov V V, Karavaev V T, Smirnova O G. Capacitor discharge welding using the pulsed magnetic resistance of welding power source. *Welding International*, 2006, **20**(2): 157-160.
- [9] Zhou Y, Dong S J, Ely K J. Weldability of thin sheet metals by small-scale resistance spot welding using high-frequency inverter and capacitor-discharge power supplies. *Journal of Electronic Materials*, 2001, **30**(8): 1012-1020.
- [10] Salzer T E. Optimizing projection welding for hermetic sealing. *Welding Journal*, 2004, (3): 42-46.
- [11] ThyssenKrupp VDM. Nicrofer 6025 HT – alloy 602 CA, Material Data Sheet No.4037, Edition: 2-5. October 2002.
- [12] Turan S, Bucklow I A, Wallach E R. Capacitor-discharge joining of oxide ceramics. *Journal of the American Ceramic Society*, 1999, **82**(5): 1242-1248.